Crystallization of Polyethylene Blends under Shear Flow. Effects of Crystallization Temperature and Ultrahigh Molecular Weight Component

Go Matsuba,* Shinya Sakamoto, Yoshiko Ogino, Koji Nishida, and Toshiji Kanaya*

Institute for Chemical Research, Kyoto University, Gokasho, Uji, Kyoto-fu 611-0011, Japan

Received December 12, 2006; Revised Manuscript Received May 10, 2007

ABSTRACT: We performed small-angle X-ray scattering (SAXS) measurements on crystallization processes of polyethylene blends of low molecular weight and ultrahigh molecular weight components with various blending ratios in order to clarify effects of ultrahigh molecular component on shish-kebab structure formation. Anisotropic scattering patterns due to kebab structure formation were observed above a certain concentration of ultrahigh molecular weight polyethylene. The critical concentration was about ∼0.1 wt % independent of the crystallization temperature below 125 °C, while it increased with the crystallization temperature above 125 °C. Analyzing the correlation between ultrahigh molecular weight component concentration and crystallization temperature in more detail, these results suggest that both the crystallization rate and the relaxation rate of the ultrahigh molecular weight component have significant effects on the shish-kebab formation process.

1. Introduction

Polyethylene is a widely used semicrystalline polymer with a range of applications in packaging, sporting goods, and some biomedical uses. Crystallinity and morphological features of polyethylene are probably the most important factors affecting the properties.[1,2] When semicrystalline polymers crystallize under shear or elongational flow, crystallization rate is enhanced, and the so-called "shish-kebab" structure can be observed in many kinds of polymers.[2−11] The shish-kebab structure, which is quite different from the spherulite in quiescent state, consists of the long central fiber core (shish structure) and surrounded by lamella crystal (kebab structure) periodically attached along the shish structure. It is believed that the shish structure is formed from extended chain crystal and the kebab is folded chain lamella crystal which grows in the direction normal to the shish structure. Elucidation of the shish-kebab structure formation process is one of the important unanswered questions in polymer physics and materials science.

Owing to recent developments of advanced characterization techniques, many studies have been carried out about polymer crystallization under flows such as shear flow, elongation flow, and mixed flow using in-situ small-angle and wide-angle X-ray scattering,[12−24] small-angle light scattering techniques,[25] optical microscopy,[25−29] atomic force microscopy (AFM), and transmission electron microscopy (TEM).[30−32] From a rheological point of view, some reports discussed the effects of shear rate[24,27,32] and/or quenching depth[33] on crystallization under shear flow. These extensive studies have provided a lot of fruitful information on the shish-kebab structure and the formation process. In spite of the efforts, however, there still remain many unsolved problems in the shish-kebab formation, especially the shish structure formation. One of the reasons is that there exist many parameters that affect the shish-kebab formation such as shear rate, shear strain, crystallization temperature, molecular weight, molecular weight distribution, and so on.

* Corresponding authors: Tel (+81)-774-38-3142; Fax (+81)-774-38-3146; e-mail gmatsuba@scl.kyoto-u.ac.jp (G.M.), kanaya@scl.kyoto-u.ac.jp (T.K.).

In a previous work, we have studied crystallization of polyethylene (PE) blends of low molecular weight and ultrahigh molecular weight (UHMW) components under shear flow using time-resolved depolarized light scattering (DPLS) techniques[34] to elucidate effects of UHMW component on the shish-kebab formation and found that the streaklike scattering normal to the flow direction, which must correspond to the shish or the shishlike structure, was observed above a certain critical concentration of UHMW PE. The critical concentration is 2−3 times larger than the chain overlap concentration $C^*_{R_g}$, suggesting that entanglements of UHMW PE chains have a significant influence on the shish-kebab structural formation. In the DPLS measurements we observed the shishlike structure on a micron scale. On the other hand, the kebab structure is on the nanometer scale.[35] In this work, therefore, we have investigated the crystallization process of PE blends of low molecular weight and UHMW components under shear flow using the time-resolved SAXS technique to observe the shish-kebab structure in nanometers, focusing on the kebab formation. One of the aims in the present study is to clarify the effect of UHMW component on the shish-kebab formation process under shear flow as a function of the concentration and the crystallization temperature and hence to resolve the shish-kebab structural formation mechanism.

2. Experimental Section

In this experiment we used two PEs with molecular weight M_w = 58 600 and ultrahigh molecular weight (UHMW) M_w = 2 000 000, and the polydispersities were M_w/M_n = 8 and 12, respectively, where M_w and M_n are the weight-average and number-average molecular weights, respectively. The fraction of the UHMW PE was in the range 0−2 wt %. These blends were prepared with a coprecipitation method. Both PEs were dissolved in xylene solution at 120 °C and stirred for 4 h, and the solution was then poured into methanol to precipitate the blend. After filtering, the obtained blend was washed with clean methanol and dried in a vacuum oven for 2 days before use. The blends were hot-pressed at 190 ± 1 °C to form films about 100 μm thick and then quenched to room temperature. The DSC measurements were carried out to characterize the thermal properties of the samples using Perkin-Elmer Diamond DSC. The DSC scans were performed under a

10.1021/ma062842+ CCC: $37.00
Published on Web 09/07/2007

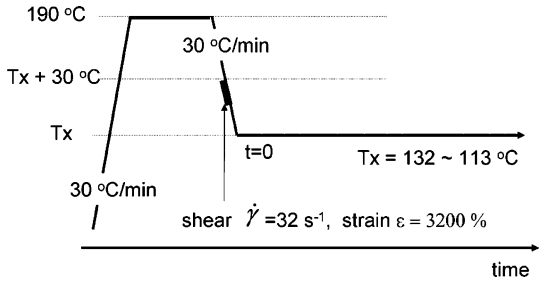

Figure 1. Temperature protocol for the shear crystallization experiments of PE blends.

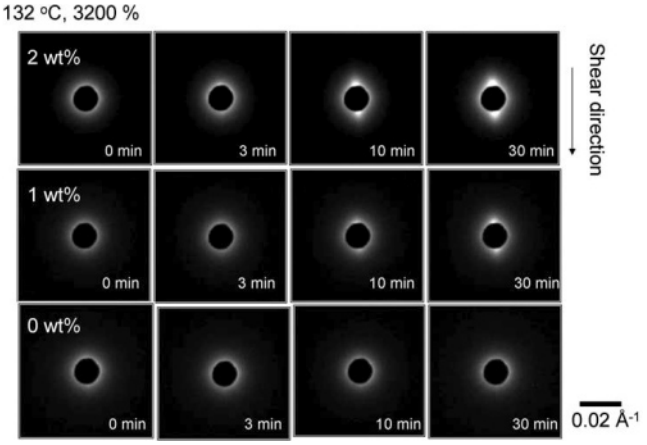

Figure 2. Time evolution of 2D SAXS images during crystallization process of PE blends with UHMW PE concentration of 0, 1, and 2 wt % at crystallization temperature 132 °C. The scale bar is $q = 0.02$ Å^{-1}. Intensity in the image is normalized to the highest intensity in the 2 wt % blend.

nitrogen environment. Both of the melting temperatures of UHMW PE and low molecular weight PE were 133 °C in the DSC measurements at heating rate of 5 °C/min.

The time-resolved small-angle X-ray scattering (SAXS) measurements were carried out using apparatus installed at the beamline BL-15A in Photon Factory, KEK, Tsukuba, Japan. The wavelength λ of the incident X-ray beam was 1.54 Å, and the camera length was 2.1 m for SAXS measurements. The SAXS intensities were detected by a CCD camera (C4880: Hamamatsu Photonics K.K.) with an image intensifier. The range of length of scattering vector q in the SAXS measurements was 0.008−0.15 Å^{-1}, where q is given by $q = 4\pi \sin\theta/\lambda$ (2θ being scattering). A Linkam CSS-450 shear cell was used to control shear field and thermal history of the polymer samples. The blend sample with thickness of 300 μm was placed between two stainless parallel plates with windows of Kapton 50 μm thick. The temperature protocol for the shear experiments is shown in Figure 1: (a) the polymer blend sample was heated up to 190 °C from room temperature at a rate of 30 °C/min, (b) held at 190 °C for 7 min, (c) cooled to the crystallization temperature $T_x = 132-116$ °C at a rate of 30 °C/min, and then (d) held at crystallization temperature T_x for the isothermal measurements. The polymer melt was subjected to pulse shear for 1 s at 30 °C above the crystallization temperature T_x. The shear rate and shear strain were 32 s^{-1} and 3200%, respectively, for all the measurements.

3. Results and Discussion

Figure 2 shows examples of time evolution of 2D SAXS profiles for the PE blends including 0, 1, and 2 wt % UHMW PE during the crystallization process at $T_x = 132$ °C after applying shear flow. In the case of 0 wt %, only isotropic scattering patterns were observed. On the other hand, the 1 and 2 wt % blends show meridional spots parallel to the shear direction, and the spots became stronger in intensity with

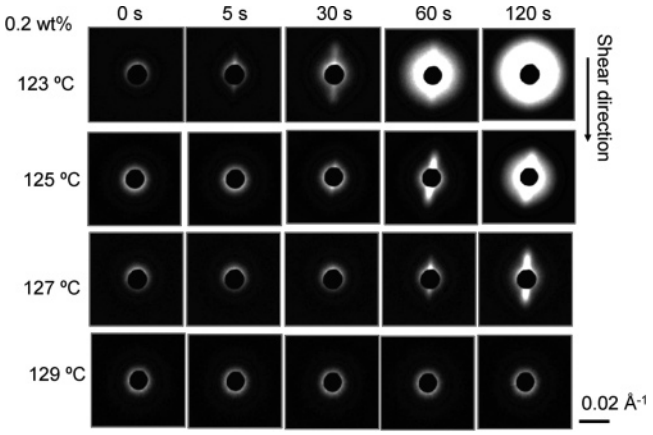

Figure 3. Time evolution of 2D SAXS images during crystallization process of PE blends at various crystallization temperatures, 123, 125, 127, and 129 °C for the UHMW PE concentration 0.2 wt %.

annealing time, suggesting that the UHMW PE enhances the anisotropic structure formation. The spot scattering appeared at around 3 min after reaching T_x for the 2 wt % blend while it appeared at ~10 min for the 1 wt % blend. This means that the crystallization rate in the PE blend increases with the UHMW PE concentration. These orientated features must be due to the kebab structures, which are oriented perpendicularly to the shear direction, and the spot position corresponds to the so-called long period between kebabs. As reported in our previous paper,[34] the UHMW PE enhances the formation of the shishlike structure, and there is a critical UHMW PE concentration for anisotropic structure formation in the DPLS measurements. The present results suggest that the UHMW PE also enhances the kebab structure formation, and there is a critical concentration for the kebab formation. This problem will be quantitatively discussed later.

It should be noted that no equatorial scattering was observed for all UHMW PE concentrations in the SAXS measurements. Equatorial streak scattering patterns are usually interpreted as a sign of shish structure.[14,18−20] Does the present result mean that no shish structure was formed during the crystallization process? In our previous report,[34,35] we found that the micron scale shishlike structure was observed as equatorial streaklike scattering in 2D DPLS measurements in similar temperature and shear conditions with the SAXS measurements. This result suggests that there should be shishlike structure even though streaklike scattering normal to the flow was not observed in the SAXS measurements. Furthermore, we studied an elongated PE blend of deuterated low molecular weight PE and protonated UHMW PE (97.2/2.8 by weight) using small-angle neutron and small-angle X-ray scattering (SANS and SAXS) and observed equatorial streaklike scattering in the SANS measurement but not in the SAXS one. In the SANS measurements, the scattering contrast is very high because of the large difference of scattering length between deuterium and proton,[36] and this directly shows that shish structure exists even if the SAXS measurement does not detect the equatorial streaklike scattering. Therefore, we will discuss the experimental results assuming that shishlike structure is formed in the measurements.

We also examined the crystallization temperatures T_x dependence of the time-resolved SAXS data. Figure 3 shows the time evolution of 2D SAXS images of a PE blend with UHMW PE concentration of 0.2 wt % for various crystallization temperatures T_x. In a temperature range below $T_x \sim 127$ °C strong meridional spots parallel to the shear direction were observed after a certain induction time and followed by isotropic scattering

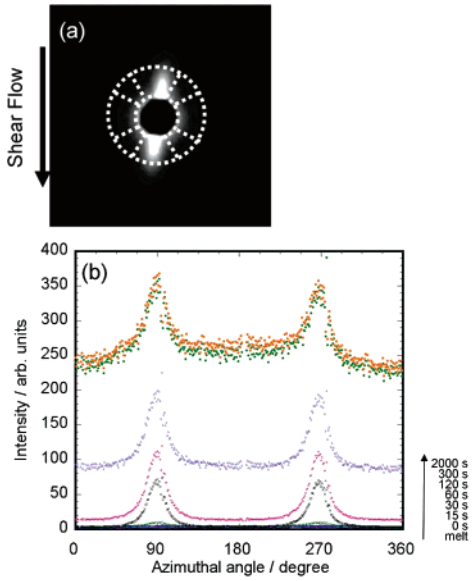

Figure 4. (a) 2D SAXS image for PE blend with UHMW PE concentration 0.2 wt % crystallized at 125 °C for 40 s. (b) Time evolution of integrated intensity in the q range between 0.008 and 0.02 Å^{-1} vs azimuthal angle. The data are the same as (a).

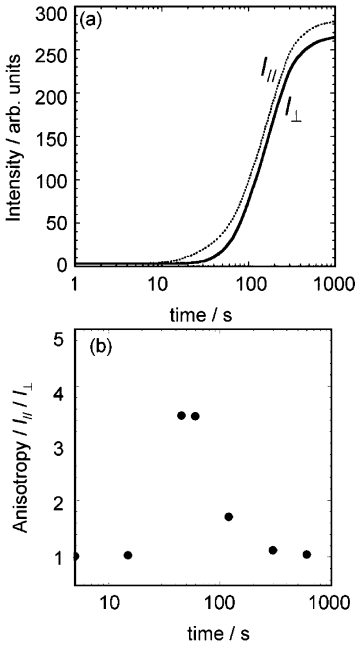

Figure 5. (a) Annealing time dependence of integrated scattering intensity parallel ($I_{||}$) and normal ($I_{\perp}$) to the shear direction. (b) Anisotropy ($I_{||}/I_{\perp}$) for PE blend with UHMW PE concentration 0.2 wt % as a function of annealing time at 125 °C.

due to the spherulite formation. As the crystallization temperature decreases, the onset time of the anisotropic scattering becomes shorter. This is due to the increase in degree of supercooling (or quenching depth), which is a driving force of crystallization in this temperature region.[37] On the other hand the meridional spots parallel to the shear direction were not observed above $T_x \sim 129$ °C, at least during the annealing period of 1 h. Note that the meridional spots were observed even above ~129 °C for the concentrations of UHMW PE higher than 0.2 wt %, showing that the critical UHMW PE concentration for the anisotropy exists and depends on the crystallization temperature.

In order to analyze the anisotropic scattering patterns, we defined degree of anisotropy. Figure 4a shows a typical

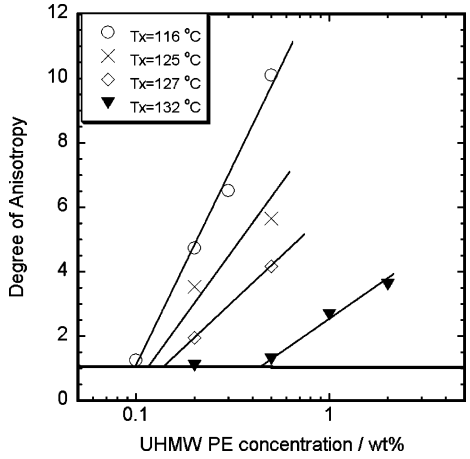

Figure 6. Degree of anisotropy as a function of UHMW PE concentration for various crystallization temperatures T_x.

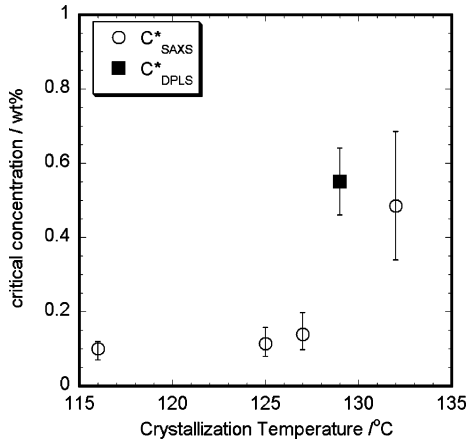

Figure 7. Critical concentration for SAXS measurement, C^*_{SAXS}, and DPLS measurement, C^*_{DPLS}, against crystallization temperature T_x.

anisotropic 2D SAXS pattern for the 0.2 wt % PE blend crystallized at $T_x = 125$ °C for 40 s after applying pulse shear. Figure 4b shows the azimuthal angle distribution of SAXS intensity integrated in a range of 0.008 Å^{-1} < q < 0.02 Å^{-1}, which is shown by dotted lines in Figure 4a. During the first 30 s the meridional intensity at around 90° and 270° increases with annealing time due to the growth of oriented kebab structure. After 1 min, on the other hand, the anisotropic intensity almost leveled off, and the isotropic intensity independent of the azimuthal angle began to increase with annealing time. This is caused by growth of isotropic spherulites.

Figure 5a shows the time evolution of integrated intensities normal ($I_{\perp}$) and parallel ($I_{||}$) to the shear flow in a range of azimuthal angle of 60° to 120° and −30° to 30°, respectively. As expected from Figure 4b, the integrated scattering intensity $I_{||}$ rises up earlier than $I_{\perp}$. The ratio of $I_{||}$ to $I_{\perp}$ is shown in Figure 5b as a function of the annealing time. The ratio $I_{||}/I_{\perp}$ has a maximum in the early stage of crystallization and decreases with time to reach unity, which means that the scattering intensity from isotropic spehrulites is quite strong compared to that from the oriented kebab structure. We defined the maximum of the ratio as the degree of anisotropy A_{aniso} in this paper and plotted in Figure 6 against logarithm of the UHMW PE concentration for various crystallization temperatures T_x. In the low concentration range, the degree of anisotropy is almost unity at each T_x while it begins to increase at a certain critical concentration, depending on the crystallization temperature T_x. Extrapolating the linear relationship to unity, we have evaluated the critical UHMW PE concentration C^*_{SAXS} for the anisotropy. The critical

UHMW PE concentration C^*_{SAXS} thus obtained is plotted against the crystallization temperature in Figure 7. In the low crystallization temperature region below about 125 °C the critical concentration is almost independent of T_x while it begins to increase above about 125 °C.

In the previous DPLS experiments[34] we showed that the critical concentration of UHMW PE, C^*_{DPLS} for the shishlike structure formation was about 0.5−0.6 wt % at $T_x = 129$ °C, which is almost identical with the C^*_{SAXS} value determined from the kebab formation. This result supports the idea that the shishlike structure exists although it is not observed in the SAXS measurements, and the kebab orientation may be dominated by the shish.

The value of C^*_{SAXS} is compared with the so-called chain overlap concentration of UHMW PE $C^*_{R_g}$, which is defined as a concentration above which random coils of UHMW PE with radius of gyration R_g begin to overlap.[38] It is given by

$$C^*_{R_g} = \frac{M_w}{(4/3)\pi\langle R_g^2\rangle^{3/2} N_A} \quad (1)$$

where $\langle R_g^2\rangle$ is the mean-square radius of gyration of UHMW PE, which is given by eq 2 under the Gaussian chain approximation with molecular weight distribution $U = M_w/M_n - 1$[39]

$$\langle R_g^2\rangle = \frac{bL(2U+1)}{3(U+1)} \quad (2)$$

where b and L are the persistence length and the contour length. Taking the literature data $[\langle R_g^2\rangle/M_w]^{1/2} = 0.46$,[40] we have calculated $C^*_{R_g}$ to be 0.209 wt %. The critical concentration for the shishlike structure at 129 °C observed in DPLS measurements[34] (0.5−0.6 wt %) was enough above $C^*_{R_g}$. Hence, we considered in the previous paper[34] that the entanglements of UHMW PE played an important role in the shishlike structure formation. The critical concentration C^*_{SAXS} (0.4−0.5 wt %) for the kebab formation at 132 °C is almost identical with this value, supporting that the entanglements of UHMW PE are substantial for the formation of the shish as well as the kebab. In this experiment, on the other hand, we observed that the critical concentration C^*_{SAXS} decreased with the crystallization temperature T_x and reached a constant value of ∼0.1 wt % below 125 °C, which is about half of the overlap concentration $C^*_{R_g}$. Does this result mean that the critical concentration is not related to entanglements? Seki et al.[27] studied a critical concentration for the anisotropic structure formation in isotactic polypropylene blend including a small amount of UHMW component and found that it was lower than the overlap concentration $C^*_{R_g}$, similar to the present result at the low crystallization temperatures below about 127 °C. In order to understand their results and our results, we have to consider the molecular weight distributions of UHMW PE as well as LMW PE. The longer chains in UHMW PE could be entangled at lower concentration than that for the average molecular weight with support of LMW PE[41,42] and hence more oriented than the shorter ones. This may be a possible reason for the lower critical concentration than the overlap concentration.

Next we will discuss the crystallization temperature dependence of the critical concentration C^*_{SAXS} for the anisotropy. For a help to the explanation we illustrated crystallization processes schematically in Figure 8 for UHMW PE concentrations below, near, and above $C^*_{R_g}$. In the case of $C_{UHMW} \sim C^*_{R_g}$ we described the crystallization process at two low and high crystallization temperatures, namely, 116 and 132 °C. In this discussion we consider two processes in the crystallization under shear flow separately. One is the orientation process of polymer chains by shear flow, and the other is the successive crystallization process, both of which must compete with the orientation relaxation of polymer chains. In order to produce the shishlike structure and the successive kebab UHMW PE must be extended and oriented due to the shear. If UHMW PE is isolated in the blend without entanglements below $C^*_{R_g}$ in Figure 8(a-1), they are somewhat extended by the shear flow (Figure 8(a-2)), however not so remarkably because the shear stress is not transmitted through the entanglements (Figure 8(a-3)). After relaxation, isotropic crystal growth was observed as shown in Figure 8(a-4). On the other hand, when the concentration of UHMW PE is above a threshold for entanglements (near $C^*_{R_g}$) as shown in Figure 8(b-1,c-1), the chains must be extended due to the connectivity as polymer network is deformed as shown in Figure 8(b-2,c-2). The threshold for the anisotropy must correspond to the concentration above which entanglements work effectively. The orientation process competes with the relaxation of UHMW PE. If the relaxation rate is faster than the shear rate, polymer chains cannot remain extended or oriented. This relaxation process must be the so-called reptation motion and/or the segmental motion[43] whose relaxation times are respectively give by

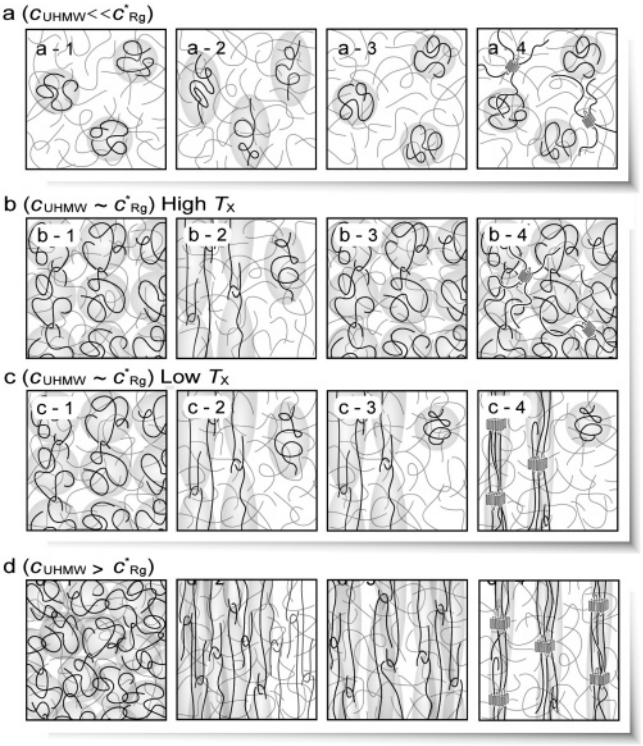

Figure 8. Schematic drawing for crystallization processes of PE blends with UHMW PE concentrations below (a), near (b, c), and above (d) $C^*_{R_g}$. In the case of $C_{UHMW} \sim C^*_{R_g}$ the crystallization processes at two low and high crystallization temperatures, namely, 132 °C (b) and 116 °C (c), are illustrated.

$$\tau_r = \tau_e Z^{3.4} = \tau_e \left(\frac{M_w}{M_e}\right)^{3.4} \quad (3)$$

$$\tau_R = \tau_e Z^2 = \tau_e \left(\frac{M_w}{M_e}\right)^2 \quad (4)$$

where τ_e and M_e are relaxation time of bond orientation and molecular weight between molecular entanglements. At the moment it is not obvious which mode is dominant for the relaxation. In a previous depolarized light scattering experiment on the same PE blends[34] we found that the very long relaxation process (approximately several seconds, depending on temperature and shear conditions) dominated the anisotropic shishlike structure formation in the crystallization after pulse shear, suggesting that the reptation motion is dominant in the relaxation process here in the discussion. The relaxation time of the reptation motion for PE with $M_w = 2\,000\,000$ at 116 °C was calculated on the basis of the reported data by Raju et al.,[44] which is ~400 s for bulk. Taking into the effect of dilution in LMW PE, it is ~0.1 s.[42] The relaxation rate for the reptation motion or the inverse of relaxation time (10 s^{-1}) is slower than the shear rate (32 s^{-1}), meaning that the relaxation process does not give significant effects on the orientation process. It is therefore expected that the initial orientation of UHMW PE is dominated by the shear rate rather than the chain relaxation, at least under the present shear and temperature conditions.

After the initial orientation by the shear the extended chains must crystallize before the chain relaxation to form the anisotropic structure such as the shish and the kebab. Both the crystallization rate (especially, crystal nucleation rate) and the relaxation rate depend on temperature. The temperature dependence of crystal nucleation rate ν_{nuc} could be described as[45]

$$\nu_{nuc} \approx \exp\left(- \frac{k\sigma^3 {v_m}^2}{kT(\Delta h_m^f)^2 (T_m^\infty - T)^2} \right) \quad (5)$$

where σ, v_m, Δh_m^f, and T_m^∞ denote the excess free energy per unit area of the surface of the nucleus, the monomer volume, the heat fusion per monomer, and the equilibrium melting temperature, respectively. According to eq 5, the crystal nucleation rate is very slow near the equilibrium melting temperature ($T_m^\infty = 142$ °C)[46,47] while it increases rapidly with being away from the equilibrium melting temperature. In this experiment the crystal nucleation rate at 116 °C is faster than that at 132 °C by a factor ~10^3. The temperature dependence of the relaxation rate (or the inverse of relaxation time) due to the reptation can be described by Williams−Landel−Ferry (WLF) equation[48]

$$1/\tau_r \sim \exp(2.303C_1(T - T_0)/(T - T_0 + C_2)) \quad (6)$$

The temperature dependence of the relaxation rate is not so large in the temperature range of this experiment. Taking the reference temperature $T_0 = 148$ K,[48] the relaxation rate at 132 °C is only 1.33 times faster than that at 116 °C. On the basis of the temperature dependence of the crystal nucleation rate as well as the relaxation rate, we can provide the following picture for the crystallization of PE at a temperature range between 116 and 132 °C under the shear flow. At high temperatures near 132 °C, the crystal nucleation rate is very slow and the relaxation rate is slightly fast compared with 116 °C, and hence extended polymer chains would relax before crystallization at around $C^*_{R_g}$, as illustrated in Figure 8(b-3,b-4).

As the crystallization temperature decreases, for example from 132 to 116 °C, the crystallization rate increases very rapidly and the relaxation rate slightly decreases. Therefore, the extended polymer chains can crystallize immediately after the initial orientation (see Figure 8(c-3,c-4)). In such temperature range the anisotropic structure formation depends only on the initial orientation which is mainly determined by the shear rate and the UHMW PE concentration, but not by the crystallization temperature. Hence, the critical shear rate is independent of temperature in this range. This corresponds to the temperature range below about 125 °C. However, as the UHMW PE concentration increases, the number of entanglements increases, and hence the degree of initial orientation increases and the relaxation rate decreases. Therefore, above a certain critical concentration above $C^*_{R_g}$, anisotropic structure is formed even at 132 °C. This is shown in Figure 8(d-3,d-4). In other words, the critical concentration of UHMW PE for the anisotropic structure formation increases with temperature. This picture qualitatively explains the present result that the critical concentration increases with crystallization temperature near the melting temperature.

4. Conclusion

In this study we performed time-resolved SAXS measurements on PE blends with various ratios of low molecular weight and UHMW components for the elucidation of shish-kebab structure formation process. It was found that there existed a critical UHMW PE concentration for anisotropic structural formation C^*_{SAXS}. Above the critical UHMW PE concentration, the kebab formation process could be observed with time-resolved SAXS measurements. The critical UHMW PE concentration is almost independent of the low crystallization temperature below 125 °C at the shear rate of 32 s^{-1} and shear strain of 3200%, while it increases with the crystallization temperature above 125 °C under the same shear condition. The key to understand the results must be the difference of temperature dependence between the crystallization rate and the relaxation rate of UHMW PE chains and the competition between them. In the temperature range of this experiment (116−132 °C), the crystallization rate at the low temperature (116 °C) is ~1000 times faster than that at the high-temperature (132 °C) while the relaxation rate at 116 °C is slower than that at 132 °C only by a factor of 1.33. Therefore, at the low temperature (116 °C) crystallization occurs immediately after the initial orientation by the shear flow before the chain relaxation, but at the high temperature (132 °C) the UHMW PE chains can relax before the crystallization near the chain overlap concentration. Hence, in order to prevent the chain relaxation and form anisotropic structure at the high temperature (132 °C), the critical concentration of UHMW PE must be higher than that at the low temperature (116 °C) to increase the number of entanglements.

References and Notes

(1) Mandelkern, L. *Crystallization of Polymers*, 2nd ed.; Cambridge University Press: Cambridge, UK, 2002.
(2) Schulz, J. M. *Polymer Crystallization*; Oxford University Press: New York, 2001.
(3) Ward, I. M. *Structure and Properties of Oriented Polymers*; Wiley: New York, 1975.
(4) Ziabicki, A. *Fundamentals of Fiber Formation*; Wiley: New York, 1976.
(5) Walczak, Z. K. *Processses of Fiber Formation*; Elsevier: Amsterdam, 2002.
(6) Keller, A.; Kolnaar, J. W. H. In *Processing of Polymers*; Meijer, H. E. H., Ed.; VCH: New York, 1997; pp 189−268.
(7) Pennings, A. J.; Kiel, A. M. *Kolloid Z. Z. Polym.* **1965**, *205*, 160−162.
(8) Pennings, A. J. *J. Polym. Sci., Part C: Polym. Symp.* **1977**, *59*, 55−86.
(9) Odell, J. A.; Grubb, D. T.; Keller, A. *Polymer* **1978**, *19*, 617−626.
(10) Bashir, Z.; Odell, J. A.; Keller, A. *J. Mater. Sci.* **1984**, *19*, 3713−3725.
(11) Bashir, Z.; Odell, J. A.; Keller, A. *J. Mater. Sci.* **1986**, *21*, 3993−4002.

(12) Gutierrez, M.-C. G.; Alfonso, G. C.; Rickel, C.; Azzurri, F. *Macromolecules* **2004**, *37*, 478−485.
(13) Dikovsky, D.; Marom, G.; Avila-Orta, C. A.; Somani, R. H.; Hsiao, B. S. *Polymer* **2005**, *46*, 3096−3104.
(14) Schultz, J. M.; Hsiao, B. S.; Samon, J. M. *Polymer* **2000**, *41*, 8887−8895.
(15) Murthy, N. S.; Grubb, D. T.; Zero, K. *Macromolecules* **2000**, *33*, 1012−1021.
(16) Ran, S.; Burger, C.; Feng, D.; Zong, X.; Crug, S.; Chu, B.; Hsiao, B. S.; Bubeck, R. A.; Yabuki, K.; Teramoto, Y.; Martin, D. C.; Johnson, M. A.; Cunniff, P. M. *Macromolecules* **2002**, *35*, 433−439.
(17) Li, L.; de Jeu, W. H. *Adv. Polym. Sci.* **2005**, *181*, 175−299.
(18) Hsiao, B. S.; Yang, L.; Somani, R, H.; Avila-Orta, C. A.; Zhu, L. *Phys. Rev. Lett.* **2005**, *94*, 117802−1-117802−4.
(19) Somani, R. H.; Yang, L.; Zhu, L.; Hsiao, B. S. *Polymer* **2005**, *46*, 8587−8623.
(20) Somani, R. H.; Yang, L.; Hsiao, B. S.; Agarwal, P. K.; Fruitwala, H. A.; Tsou, A. H. *Macromolecules* **2002**, *35*, 9096−9104.
(21) Kumaraswamy, G.; Verma, R. K.; Kornfield, J. A.; Yeh, F.; Hsiao, B. S. *Macromolecules* **2004**, *37*, 9005−9017.
(22) Zhu, P.-w.; Edward, G. *Polymer* **2004**, *45*, 2603−2613.
(23) Stribeck, N.; Camarillo, A. A.; Cunis, S.; Bayer, R. K.; Gehrke, R. *Macromol. Chem. Phys.* **2004**, *205*, 1445−1454.
(24) Heeley, E. L.; Fernyhough, C. M.; Graham, R. S.; Olmsted, P. D.; Inkson, N. J.; Embery, J.; Groves, D. J.; McLeish, T. C. B.; Morgovan, A. C.; Meneau, F.; Bras, W.; Ryan, A. J. *Macromolecules* **2006**, *39*, 5058−5071.
(25) Pogodina, N. V.; Lavrnenko, V. P.; Srinivas, S.; Winter, H. H. *Polymer* **2001**, *42*, 9031−9043.
(26) Kornfield, J. A.; Kumaraswamy, G.; Issian, A. M. *Ind. Eng. Chem. Res.* **2002**, *41*, 6383−6392.
(27) Seki, M.; Thurman, D. W.; Oberhauser, J. P.; Kornfield, J. A. *Macromolecules* **2002**, *35*, 2583−2594.
(28) Wang, J.; Kuang, X.; Yan, S. *J. Polym. Sci., Part B: Polym. Phys.* **2004**; *42*, 2703−2709.
(29) Azzurri, F.; Alfonso, G. C. *Macromolecules* **2005**, *38*, 1723−1728.
(30) Nakae, M.; Uehara, H.; Kanamoto, T.; Zacharides, A. E.; Porter, R. S. *Macromolecules* **2000**, *33*, 2632−2641.
(31) Koike, Y.; Cakmak, M. *J. Polym. Sci., Part B: Polym. Phys.* **2004**, *42*, 2228−2237.
(32) Bent, J.; Hutching, L. R.; Richards, R. W.; Gough, T.; Spares, R.; Coates, P. D.; Grillo, I.; Harlen, O. G.; Read, D. J.; Graham, R. S.; Likhtman, A. E.; Groves, D. J; Nicholson, T. M.; McLeish, T. C. B. *Science* **2003**, *301*, 1691−1695.
(33) Coppola, S.; Balzono, L.; Gioffredi, E.; Maffettone, P. L.; Grizzuti, N. *Polymer* **2004**, *45*, 3249−3256.
(34) Ogino, Y.; Fukushima, H.; Matsuba, G.; Takahashi, N.; Nishida, K.; Kanaya, T. *Polymer* **2006**, *47*, 5669−5677.
(35) Ogino, Y.; Fukushima, H.; Takahashi, N.; Matsuba, G.; Nishida, K.; Kanaya, T. *Macromolecules* **2006**, *39*, 7617−7625.
(36) Higgins, J. S.; Benoit, H. C. *Polymers and Neutron Scattering*; Oxford University Press: Oxford, 1994.
(37) Turnbull, D.; Fisher, J. C. *J. Chem. Phys.* **1949**, *17*, 71−73.
(38) de Gennes, P. G. *Scaling Concepts in Polymer Physics*; Cornel University Press: Ithaca, NY, 1979.
(39) Oberthuer, R. C. *Maklomol. Chem.* **1978**, *179*, 2693−2706.
(40) Schelten, J.; Wignall, G. D.; Vallard, D. G. H.; Schltz, W. *Colloid Polym. Sci.* **1974**, *252*, 749−752.
(41) Struglinsski, M. J.; Gassley, W. W. *Macromolecules* **1985,** *21*, 2630−2643.
(42) Watanabe, H. *Prog. Polym. Sci.* **1999**; *24*, 1253−1403.
(43) Doi, M.; Edwards, S. F. *The Theory of Polymer Dynamics*; Oxford University Press: Oxford, 1986.
(44) Raju, V. R.; Smith, G. G.; Marin, G.; Knox, J. R.; Graessley, W. W. *J. Polym. Sci., Polym. Phys. Ed.* **1979**, *17*, 1183−1195.
(45) Strobl, G. *The Physics of Polymers*; Springer-Verlag: Berlin, 1996.
(46) Kim, M. H.; Phillips, P. J.; Lin, J. S. *J. Polym. Sci., Part B: Polym. Phys.* **2000**, *38*, 154−170.
(47) Wagner, J.; Phillips, P. J. *Polymer* **2001**, *42*, 8999−9013.
(48) Brandup, J., Immergut, E. H., Grulke, E. A., Eds. *Polymer Handbook*, 4th ed.; Wiley-Interscience: New York, 1999.

MA062842+